A deletion at the X-linked ARHGAP36 gene locus is associated with the orange coloration of tortoiseshell and calico cats

Toh, Hidehiro
Medical Institute of Bioregulation, Kyushu University

Au Yeung, Wan Kin
Medical Institute of Bioregulation, Kyushu University

Unoki, Motoko
Medical Institute of Bioregulation, Kyushu University

Matsumoto, Yuki
Data Science Center, Azabu University

他

出版情報：Current Biology. 35 (12), pp.2816-2825.e3, 2025-06-23. Cell Press
バージョン：

Article

Current Biology

A deletion at the X-linked *ARHGAP36* gene locus is associated with the orange coloration of tortoiseshell and calico cats

Graphical abstract

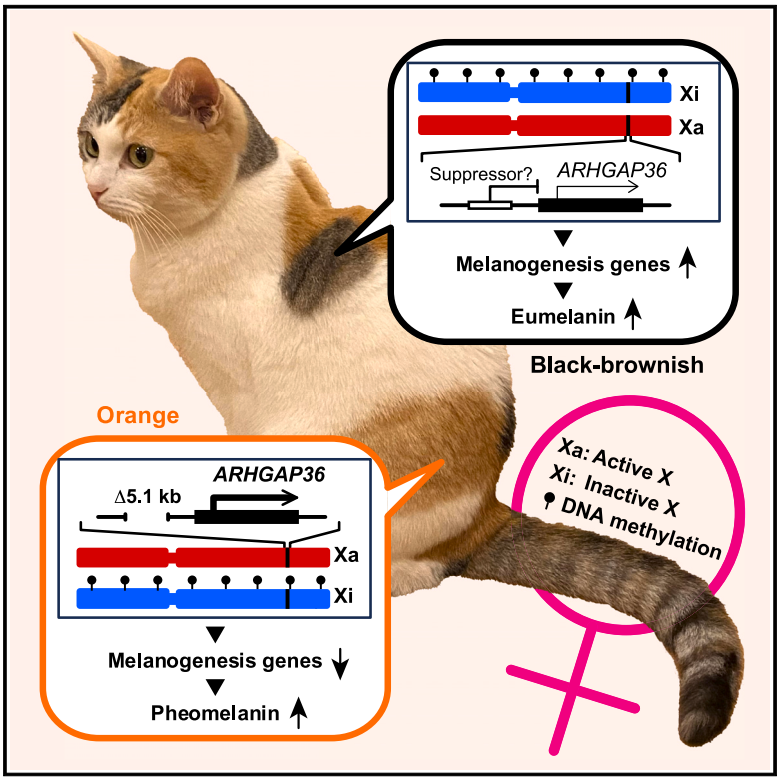

Highlights

- X-linked *ARHGAP36* is identified as the gene responsible for the orange coat of cats
- A deletion at this locus alters *ARHGAP36* expression, leading to pigment-type switch
- Evidence suggests that *ARHGAP36* is subject to random X chromosome inactivation
- The deletion seems widespread in cats, suggesting a single origin of this phenotype

Authors

Hidehiro Toh, Wan Kin Au Yeung, Motoko Unoki, ..., Yasukazu Nakamura, Miho Matsuda, Hiroyuki Sasaki

Correspondence

hsasaki@bioreg.kyushu-u.ac.jp

In brief

The X-linked orange locus is responsible for the orange coat color of domestic cats, including tortoiseshell and calico cats, and is proposed to be subject to random X chromosome inactivation. Here, Toh, Au Yeung, Unoki, et al. identify a genomic deletion that alters *ARHGAP36* expression as the causative genetic variant.

Toh et al., 2025, Current Biology *35*, 2816–2825
June 23, 2025
https://doi.org/10.1016/j.cub.2025.03.075

CellPress

CellPress
OPEN ACCESS

Current Biology

Article

A deletion at the X-linked *ARHGAP36* gene locus is associated with the orange coloration of tortoiseshell and calico cats

Hidehiro Toh,[1,2,11] Wan Kin Au Yeung,[1,3,11] Motoko Unoki,[1,4,11] Yuki Matsumoto,[5,6] Yuka Miki,[1,7] Yumiko Matsumura,[8] Yoshihiro Baba,[1] Takashi Sado,[9] Yasukazu Nakamura,[2] Miho Matsuda,[10] and Hiroyuki Sasaki[1,12,*]
[1]Medical Institute of Bioregulation, Kyushu University, Fukuoka 812-8582, Japan
[2]National Institute of Genetics, Research Organization of Information and Systems, Mishima 411-8540, Japan
[3]College of Liberal Arts, International Christian University, Mitaka 181-8585, Japan
[4]School of International Health, Graduate School of Medicine, The University of Tokyo, Bunkyo-ku, Tokyo 113-0033, Japan
[5]Data Science Center, Azabu University, Sagamihara 252-5201, Japan
[6]Research and Development Section, Anicom Specialty Medical Institute Inc., Yokohama 231-0033, Japan
[7]School of Medicine, Nagoya University, Nagoya 466-8550, Japan
[8]Inakazu Dog & Cat Kashii Hospital, Fukuoka 813-0003, Japan
[9]Graduate School of Agriculture and Agricultural Technology and Innovation Research Institute, Kindai University, Nara 631-8505, Japan
[10]Faculty of Dental Science, Kyushu University, Fukuoka 812-8582, Japan
[11]These authors contributed equally
[12]Lead contact
*Correspondence: hsasaki@bioreg.kyushu-u.ac.jp
https://doi.org/10.1016/j.cub.2025.03.075

SUMMARY

The X-linked *orange* (*O*) locus in domestic cats controls an unknown molecular mechanism that causes the suppression of black-brownish pigmentation in favor of orange coloration. The alternating black-brownish and orange patches seen in tortoiseshell and calico cats are considered classic examples of the phenotypic expression of random X chromosome inactivation (XCI) occurring in female mammals. However, the *O* gene in the cat genome has not been identified, and the genetic variation responsible for the orange coloration remains unknown. We report here that a 5.1-kilobase (kb) deletion within an intron of the X-linked *ARHGAP36* gene, encoding a Rho GTPase-activating protein, is closely and exclusively associated with orange coloration. The deleted region contains a highly conserved putative regulatory element, whose removal is presumed to alter *ARHGAP36* expression. Notably, *ARHGAP36* expression in cat skin tissues is linked to the suppression of many melanogenesis genes, potentially shifting pigment synthesis from eumelanin to pheomelanin. Furthermore, we find evidence that the gene undergoes XCI in female human and mouse cells and XCI-dependent CpG island methylation consistent with random XCI in female domestic cats. The 5.1-kb deletion seems widespread in domestic cats with orange coat coloration, suggesting a single origin of this coat color phenotype.

INTRODUCTION

The domestic cat (*Felis silvestris catus*) is a valued companion animal, a vermin-control agent, and a provider of important biomedical models that most likely descended from a wildcat progenitor subspecies, *Felis silvestris lybica*, around 10,000 years ago.[1–3] Domestic cats display a diversity of phenotypic variation, including a range of coat coloration patterns resulting from interactions between multiple genetic loci, making them excellent models for studying gene function and regulation. For example, early genetic studies on the orange phenotype of domestic cats helped to discover X-linked inheritance in mammals.[4–6]

The X-linked *orange* (*O*) locus controls an unidentified molecular mechanism that causes the suppression of black-brownish pigmentation (eumelanin) and promotion of orange coloration (pheomelanin).[7] Phenotypic variants of this locus can be seen in the tortoiseshell (mottled orange and black-brownish pattern) and the calico cats (mosaic pattern of large orange, black-brownish, and white patches), which are almost exclusively female. These coloration patterns arise as a result of X chromosome inactivation (XCI), which is an important epigenetic mechanism that equalizes X-linked gene dosage between females and males. More than 60 years ago, it was suggested by Mary Lyon that one of the two X chromosomes in a female embryo is randomly selected and inactivated in each cell during early development, and that descendant cells maintain the same inactivation pattern as the ancestral cell.[8] As a result, the alternative expression of the *orange* allele versus the wild-type allele in different skin patches creates a mosaic coloration pattern in female cats heterozygous at the *O* locus.[8] Rare occurrence of the mosaic phenotype in males can be explained by sex

CellPress
OPEN ACCESS

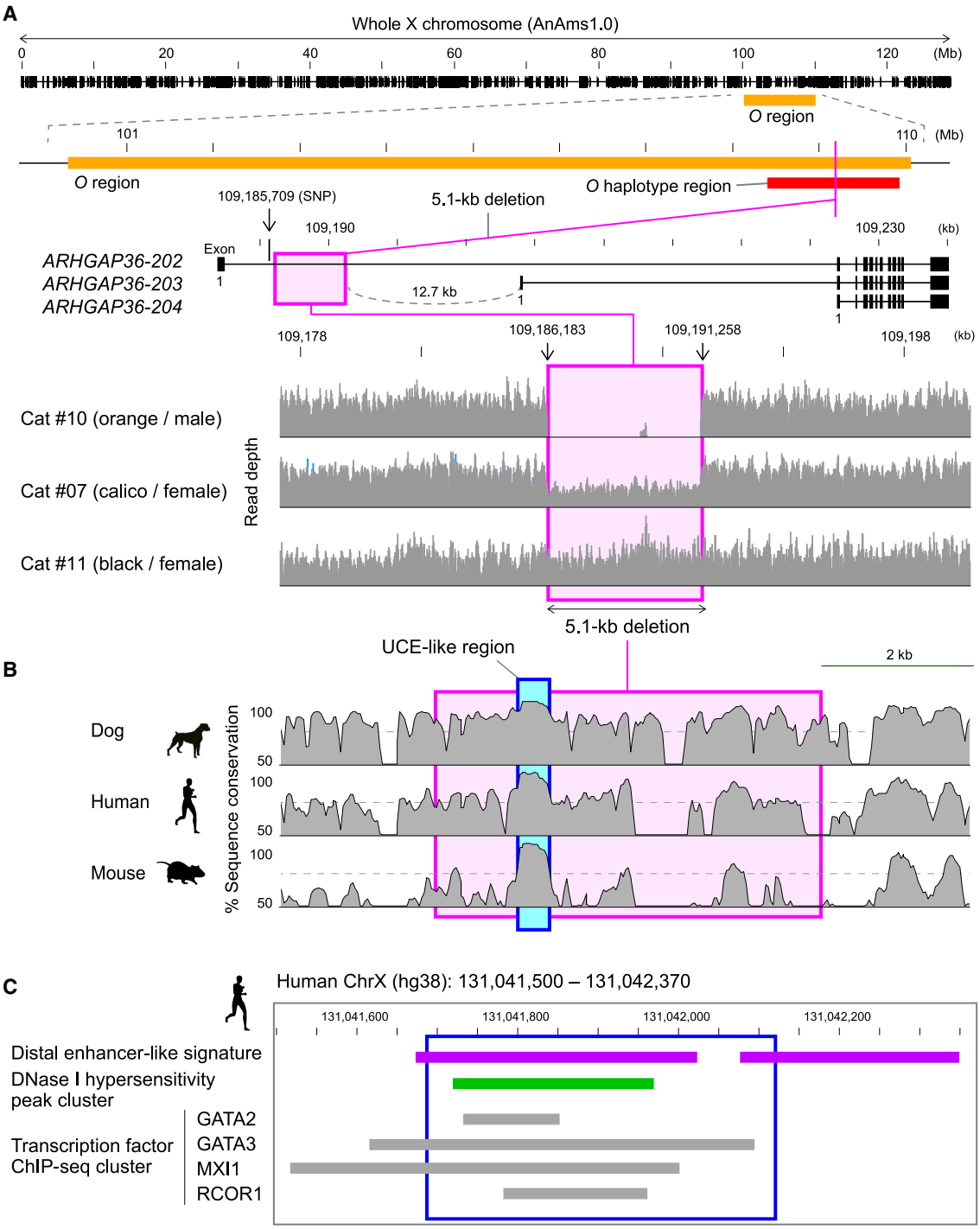

Figure 1. Identification of the 5.1-kb deletion within the *O* haplotype region

(A) Location of the 5.1-kb deletion associated with the orange coloration in the cat X chromosome. An orange bar indicates the 9.7-Mb *O* region identified using microsatellite markers,[11] and a red bar marks the 1.5-Mb *O* haplotype region identified using SNP microarray.[12] A pink box marks the 5.1-kb region deleted in cats with the orange coloration. Exon-intron structure of *ARHGAP36* is shown with exon usage generating three isoforms. Representative WGS read-depth profiles across the 5.1-kb region are shown at the bottom for three cats with indicated coat color and sex.

(B) Sequence similarity profiles of the region containing the 5.1-kb deletion. Sequence similarity between domestic cats and indicated species is shown. A pink box highlights the deleted region, while a blue box marks the UCE-like sequence.

(legend continued on next page)

chromosome aneuploidy (XXY), chimerism, mosaicism, or somatic mutations.[9]

While the coat color phenotypes of tortoiseshell and calico cats are often quoted as visually recognizable examples of XCI in female mammals, the gene and the genetic variation responsible for the orange coat color remain unknown. A previous genetic mapping study using microsatellite markers located the *O* locus within a 9.7-megabase (Mb) region of the cat X chromosome.[10,11] Haplotype analysis also suggested multiple origins for the phenotype.[11] A more recent study using a 63K DNA array identified a 1.5-Mb haplotype block associated with orange coloration within this 9.7-Mb region.[12] The study also provided a list of 12 genes located within the haplotype region as the candidates for the *O* gene; however, none were known to regulate melanin synthesis.

In this study, we searched for the gene and genetic variation associated with the orange coloration by comparing the genomic sequences of cats with orange coat color, including tortoiseshell and calico cats, and control non-orange cats. We identified a 5.1-kilobase (kb) deletion in one of the protein-coding genes located within the haplotype region, which was closely and exclusively associated with orange coloration. We further present evidence that this gene undergoes XCI, most likely random XCI, in multiple mammalian species.

RESULTS

Systematic screening for genetic variations responsible for orange coloration using WGS

To identify the genetic variation responsible for the orange coloration and X-linked *O* gene in domestic cats, we sequenced the DNA samples from 18 cats, including eight calico cats, one tortoiseshell cat, one cat with both orange and white coat regions, and eight cats without orange coat color (Tables S1 and S2; Figure S1A). We mapped the whole-genome sequencing (WGS) reads to the AnAms1.0 cat genome, a high-quality chromosome-scale sequence assembly with only one short unmapped scaffold.[9] Thirteen putative protein-coding genes, overlapping with the 12 genes previously reported,[12] were identified in the 1.5-Mb haplotype region (Table S3).

The AnAms1.0 genome was derived from a silver tabby American Shorthair[13] (Figure S1A), and we used this sequence as a reference (wild type) to identify genetic variations associated with the orange coloration. Within the 1.5-Mb haplotype region, we identified 2,569 small genetic variants, including single nucleotide polymorphisms (SNPs) and small insertions and deletions, in ten cats with orange coat color, and 2,073 variants in eight cats without it. Removal of variants shared by the two groups identified 594 small variants unique to the orange group (Figure S2A). Using published WGS data from nine cats with color photographs, contributed by the 99 Lives Cat Genome Sequencing Initiative[14] (Table S4) (photographs available in the paper or at https://cvm.missouri.edu/research/feline-genetics-and-comparative-medicine-laboratory/99-lives/successfully-sequenced-cats/), we identified 901 small variants in seven non-orange cats. After removing the variants shared with this pool, a total of 450 small variants unique to the orange group remained, none of which were frameshift, missense, or nonsense mutations in the protein-coding exons (Figure S2B).

To search for other types of variations, we analyzed the sequence depth across the 1.5-Mb *O* haplotype region and identified a 5.1-kb deletion present only in the orange cat group (Figure 1A). This deletion was located within the first intron of *ARHGAP36* and was surprisingly present in all ten sequenced cats with the orange coloration but in none of the eight cats without it (Figures 1A and S3A). Notably, the eight calico cats and one tortoiseshell cat were heterozygous for the deletion, consistent with the mosaic coat color phenotype. Furthermore, analysis of the published data from the above-described nine cats with coat color information confirmed the presence of this deletion only in those with orange coat color, namely a calico cat named Cali and her father, Orion[14] (Figure S3B; Tables S4 and S5). Again, the calico cat was heterozygous for the deletion. While we could not exclude at this stage that one of the identified small variants was responsible for the *O* allele, the consistent and exclusive presence of the deletion made it a strong candidate for the causative genetic variation. Interestingly, the SNP (positions 108,984,866 in AnAms1.0 or 110,230,748 in felCat9) (hereafter, we use the AnAms1.0 coordinate) previously found to be most closely associated with the orange coloration[15] was located in an intron of *ENOX2*, a protein-coding gene located closest to *ARHGAP36* (Table S3).

Strong association between the deletion and orange coloration

To confirm the association between the 5.1-kb deletion within an intron of *ARHGAP36* and the orange coloration, additional DNA samples (n = 40) were analyzed by polymerase chain reaction (PCR). The study showed that all six calico cats, including one rare male calico cat (#24) (Figure S1B), and all five tortoiseshell cats had the deletion in one of the two X chromosomes (Figure S3C; Table S1). The fact that the male calico was heterozygous for the deletion is consistent with the presence of sex chromosome aneuploidy (presumably XXY).[9] Three additional cats with orange but no black-brownish coat color (#30, #31, and #32) had this deletion in a hemizygous (male) or homozygous manner (female), while none of the non-orange cats did (n = 26) (Table S1). Combining our WGS and PCR data, a total of 58 cats (24 orange and 34 non-orange) demonstrated a 100% link between the deletion and the orange coloration (Tables 1 and S1). Addition of the information from the publicly available WGS data of the above-described nine photographed cats further supported this link in a total of 67 cats (26 orange and 41 non-orange).

Next, we sought to determine whether any of the 450 SNPs found only in the orange cat group were linked to the 5.1-kb

(C) ENCODE annotations for the UCE-like sequence on human chromosome X. Shown are features of the hg38 131,041,688–131,042,122 region corresponding to the cat UCE-like sequence (boxed by blue lines) and adjacent regions, retrieved from the UCSC Genome Browser. Purple bars indicate regions showing distal enhancer-like signatures, and a green bar highlights the DNase I hypersensitive site cluster identified in neuroblastoma. Gray bars represent ChIP-seq peak clusters for indicated transcription factors in neuroblastoma.
See also Figures S1–S3, and S6, and Tables S1–S3, S4, and S5.

CellPress
OPEN ACCESS

Table 1. Association between orange coloration and a 5.1-kb deletion within *ARHGAP36*

Coat color pattern	Genotype regarding the deletion[a]					
	Female			Male		
	+/+	Δ/+	Δ/Δ	+/Y	Δ/Y	Δ/+/Y
Calico	0	13	0	–	–	1
Tortoiseshell	0	6	0	–	–	–
Orange	0	0	2	0	2	–
Non-orange	16	0	0	18	0	–
Total	16	19	2	18	2	1

See also Table S1.
[a]Δ, 5.1-kb deletion; +, wild type; Y, Y chromosome.

deletion because such an SNP could also contribute to the phenotype. We found that only one SNP (C>T, at position 109,185,709), located 0.5-kb upstream of the deletion within an intron of *ARHGAP36* (Figure 1A), was present in all ten sequenced cats of our orange group (Figures S2C and S2D). We then used 258 WGS datasets, mostly from the 99 Lives Cat Genome Sequencing Initiative[14] (including those from the nine cats with color images), and found that, while all 61 cats carrying the 5.1-kb deletion (21 hemizygous males, 12 homozygous females, and 28 heterozygous females) had the SNP, none of the 197 cats without it did (Tables S4 and S5). All 28 females heterozygous for the deletion were also heterozygous for the SNP. These results indicate that the deletion and a linked SNP are present within an intron of *ARHGAP36* in cats with the orange coat coloration.

UCE-like sequence in the deleted region

We then performed a more detailed analysis of the deletion and SNP. Sanger sequencing of the PCR products confirmed a 5,076-nucleotide (nt) deletion spanning from position 109,186,183 to 109,191,258 (Figure S3D). Importantly, the deleted region contained a 436-nt sequence showing strong evolutionary conservation reminiscent of ultraconserved element (UCE)[16] (Figures 1B and S3E). According to the data from the human Encyclopedia of DNA Elements (ENCODE) project,[17] this UCE-like sequence contained a DNase I hypersensitive site cluster in human neuroblastoma cells and chromatin immunoprecipitation-sequencing (ChIP-seq) clusters for transcription factors including GATA2/3, max interactor 1, dimerization protein (MXI1), and REST corepressor 1 or CoREST (RCOR1) (Figure 1C). Interestingly, while GATA family proteins are transcriptional activators,[18] MXI1 and RCOR1 are transcriptional repressors.[19,20] Therefore, this putative *cis*-regulatory element could function as a transcriptional enhancer or a repressor. By contrast, the SNP located approximately 0.5-kb upstream of the deletion (position 109,185,709) was not in a region conserved among species, making it unlikely to have a role in gene regulation. It is likely that the 5.1-kb deletion removed a critical regulatory region, leading to altered expression of a nearby gene(s) such as *ARHGAP36*.

Negative correlation between *ARHGAP36* and melanogenesis gene expression

We hypothesized that the *O* gene would exhibit differential expression based on the presence or absence of the deletion in skin tissues, especially in orange and black-brownish coat regions. We first performed RNA sequencing (RNA-seq) on skin tissues obtained from the auricles of different adult calico cats (#19, #20, and #22, females, precise ages unknown) (Table S2). Of the 13 protein-coding genes found in the *O* haplotype region, *ARHGAP36* was expressed exclusively in the orange region, while all other genes detected in the orange region were also expressed in the black-brownish and white regions (Figures 2A and S4A). We then analyzed multiple skin tissues obtained from a young calico cat that died of unknown causes (#01, female, 3 weeks old) (Figure S1C; Table S2). *ARHGAP36* was persistently expressed in the orange regions but variably expressed in the black-brownish regions with virtually no expression in one of the samples (Figures 2A and S4A). The reason for this variability is currently unknown but could be due to differences in hair cycle stage or cell composition. *IGSF1*, a gene located next to *ARHGAP36*, behaved similarly, suggesting that the two genes might share a regulatory mechanism, although the expression level of *IGSF1* was extremely low (<0.6 fragments per kilobase of exon per million reads mapped [FPKM]) (Figure 2A). Notably, *ARHGAP36-203* was the only mRNA isoform produced in the skin samples (Figure S4B). Since the expression pattern observed in the black-brownish regions should be the wild-type pattern, the more persistent *ARHGAP36*, and possibly *IGSF1*, expression induced by the deletion could shift the pigment synthesis from eumelanin to pheomelanin in the orange regions.

Based on the publicly available gene expression databases, such as the genotype-tissue expression (GTEx),[21] both *ARHGAP36* and *IGSF1* are highly expressed in neuro-endocrinological tissues, such as the hypothalamus, pituitary gland, and adrenal gland. Notably, these tissues are rich in neural crest-derived cells, from which melanocytes also originate.[22] *IGSF1* encodes a member of the immunoglobulin superfamily, and loss-of-function mutations in this gene cause X-linked central hypothyroidism and testicular enlargement (OMIM300888).[23] There is currently no known role for *IGSF1* in hair follicle development or melanogenesis. In addition, its expression was very low in cat skin tissues as described above (Figures 2A and S4A). *ARHGAP36* encodes a member of the Rho GTPase-activating protein family, yet a systematic study has shown that it lacks GTPase-activating activity.[24] Rather, it has been reported that ARHGAP36 mediates and activates Hedgehog (HH) signaling and suppresses protein kinase A (PKA) signaling.[25–29] Importantly, the HH and PKA signaling pathways mediate hair follicle development and melanogenesis, respectively, and dysregulation of human *ARHGAP36* is implicated in X-linked Bazex-Dupré-Christol syndrome (BDCS, OMIM301845),[30] characterized by follicular atrophoderma, congenital hypotrichosis, and multiple basal cell naevi and carcinomas. Hence, its known biological roles make *ARHGAP36* an excellent candidate for the *O* gene.

To correlate the expression of *ARHGAP36* and other genes in the skin, we first excluded the data from the white regions of cat #01, where no melanogenesis is expected, and categorized the remaining four into two groups: *ARHGAP36* positive (orange 1 and 2 and black-brownish 1) and *ARHGAP36* negative (black-brownish 2). We found 341 genes showing positive correlation with *ARHGAP36* and 517 genes showing negative correlation (Table S6). Strikingly, an analysis using the Kyoto Encyclopedia of Genes and Genomes (KEGG) in the Database for Annotation,

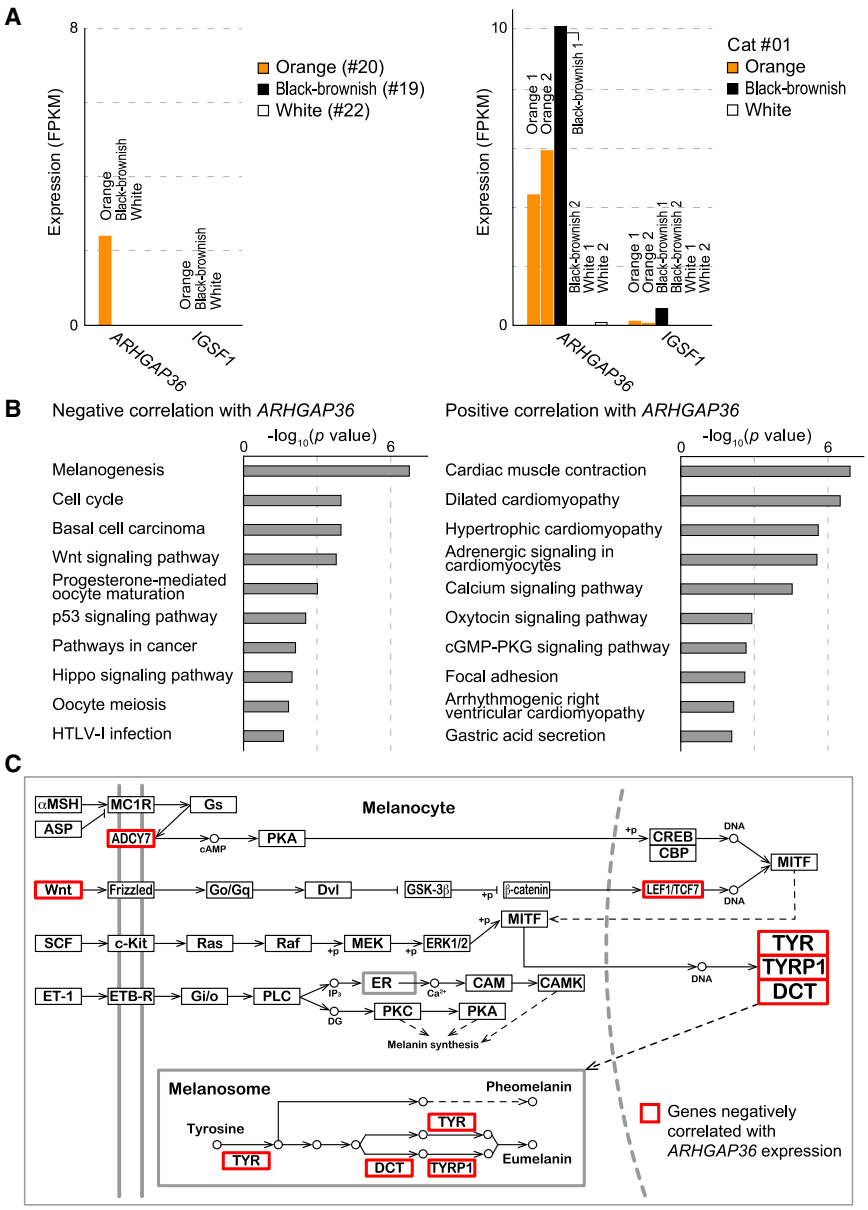

Figure 2. Negative correlation between *ARHGAP36* and melanogenesis gene expression

(A) Expression levels of *ARHGAP36* and *IGSF1* in cat auricles (left) and skin tissues (right). RNA-seq data were obtained in small auricle pieces of different coat colors derived from different cats (left) and in skin samples of different coat colors derived from a single calico cat (#01) (right).

(B) Top ten KEGG pathways in which genes negatively and positively correlated with *ARHGAP36* are enriched. The pathways are ranked by significance.

(C) KEGG diagram of the melanogenesis pathway highlighting genes negatively correlated with *ARHGAP36* expression (red boxes). The original KEGG pathway diagram was slightly modified for clarity.

See also Figures S1 and S4, and Tables S2 and S6.

Visualization, and Integrated Discovery (DAVID) system[31,32] revealed that the negatively correlated genes were enriched in the melanogenesis pathway (Figure 2B). Examples of the melanogenesis genes negatively correlated with *ARHGAP36* included *ADCY7*, *DCT*, *LEF1*, *TCF7*, *TYR*, *TYRP1*, *WNT10B*, *WNT3A*, *WNT5A*, and *WNT6*. The roles of the protein products were distributed in the whole melanogenesis pathway, from ligands activating the signaling pathways to enzymes directly involved in the melanin synthesis (Figure 2C). Notably, among the melanin synthesis enzymes, TYRP1 and DCT are involved in eumelanin synthesis but not pheomelanin synthesis. Therefore, their downregulation may attenuate eumelanin synthesis and cause a shift toward pheomelanin synthesis.[33] The negative correlation between *ARHGAP36* and melanin synthesis enzyme genes was also seen in the auricle skin samples from different calico cats (Figure S4C).

ARHGAP36 is subject to XCI in female mammalian cells

The mosaic coat color of tortoiseshell and calico cats is attributed to the random inactivation of the X-linked *O* gene in *O/o* female cells.[8] However, a proportion of X-linked genes is known to escape XCI to varying degrees.[34] We therefore wished to examine whether *ARHGAP36* of the domestic cat is subject to random XCI in female cells and whether melanocytes in black-brownish and orange regions express the different alleles. To do this, we would need tissue samples from female cats (preferably from tortoiseshell or calico cats) carrying informative SNPs within the *ARHGAP36* transcripts. However, we have not yet had a chance to access such samples.

The XCI is investigated in detail in humans and mice. One of the authors (T.S.) previously investigated the inactivation of the X-linked genes using fibroblast cells derived from female mouse embryos obtained by crossing a JF1 female and a C57BL/6J male.[35,36] In the study, the X chromosome from C57BL/6J was fixed to be active by an internal deletion of *Xist* ($X^{B6\text{-}\Delta A}$), a gene essential for XCI.[31] We reprocessed the RNA-seq data and found that all 172 SNP-containing *Arhgap36* reads were from the $X^{B6\text{-}\Delta A}$, indicating that the gene is subject to XCI in mice (Table S7). We also reprocessed the chromatin RNA-seq data from a similar study using embryonic fibroblast cells where the X chromosome from *Mus musculus castaneus* was genetically fixed to be inactive[37] and found that all *Arhgap36* transcripts were from the other X (27 reads containing informative SNPs) (Table S7). Regarding the XCI of human *ARHGAP36*, an SNP-based allelic imbalance analysis was performed for a total of 409 X-linked genes in multiple lymphoblastoid and fibroblast cells.[38] The data indicated that human *ARHGAP36* (designated *FLJ30058* in that study)

CellPress
OPEN ACCESS

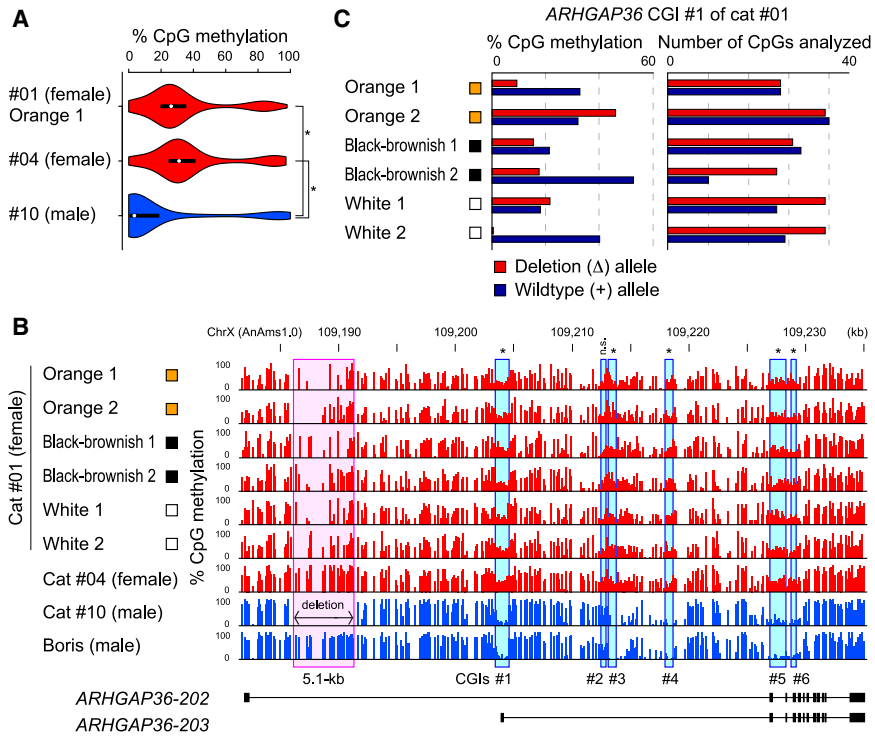

Figure 3. DNA methylation profiles of the X chromosome and *ARHGAP36* in female and male cats

(A) Violin plots comparing CpG methylation levels of 362 X-linked promoter CGIs between female and male cats. The WGBS data were from skin (cat #01, orange patch 1) and peripheral blood cells (cats #04 and #10). Circles represent the median, and box edges represent the 25th and 75th percentiles. Statistical significance was assessed using the exact Wilcoxon rank sum test, and asterisks (*) indicate $p < 2e-16$.

(B) CpG methylation profiles of the cat *ARHGAP36* region in female (red) and male cats (blue). The WGBS data were obtained from skin regions (cat #01) and peripheral blood cells (cats #04 and #10). The WGBS data of peripheral blood cells from a male cat named Boris was obtained from a publicly available dataset (SRA: SRX548709). A pink box indicates the region corresponding to the 5.1-kb deletion, and blue boxes indicate the CGIs. Differences in methylation between males and females were statistically evaluated using Fisher's exact test, and asterisks (*) indicate $p < 2e-16$.

(C) Allelic CpG methylation of CGI #1 of *ARHGAP36*. The CpG methylation levels (left) and the number of CpGs analyzed using SNP-containing WGBS reads (right) are shown. The data were from different skin regions of a calico cat (#01). Two SNPs were used to analyze allele-specific reads: *cis* association of the SNPs with the deletion (Δ) was determined using the data from cats hemizygous (males) and homozygous (females) for the deletion. Note that CGI #1 overlaps with the most active promoter in the skin (Figure S4B).

See also Figures S1 and S5, and Tables S2 and S7.

was subject to XCI in all ten female cell lines possessing informative SNPs (Table S7). These results show that, while direct evidence is lacking for domestic cats, *ARHGAP36* is subject to XCI in multiple mammalian species.

DNA methylation status of cat *ARHGAP36* is consistent with random XCI

DNA methylation can serve as a hallmark for genes that are subject to XCI, as X-linked CpG islands (CGIs), especially promoter-associated ones, are highly methylated on the inactive X but almost unmethylated on the active X.[39] Using published whole-genome bisulfite sequencing (WGBS) datasets from human and mouse tissues,[40,41] we first compared the methylation levels of the *ARHGAP36* CGIs between the sexes, which showed significantly higher methylation levels in females of both species (Figures S5A and S5B), consistent with their XCI-dependent methylation. We then investigated the published allelic methylation data from hybrid mouse embryonic fibroblast cells carrying a *Mus musculus castaneus*-derived inactive X[37] and found that the *Arhgap36* CGI is more methylated on the inactive X (Figure S5A).

To determine whether the CGIs of cat *ARHGAP36* undergo XCI-dependent methylation, we performed WGBS on skin tissues of different colors from a female calico cat (#01) and peripheral blood cells from two other cats (female #04 and male #10) (Table S2). We also obtained publicly available data from a male cat named Boris.[42] Globally, X-linked promoter CGIs (n = 362) were more methylated in females (#01 and #04) (the interquartile range 20%–41% methylation [median 26.3% and 31.2%, respectively]) than in a male (#10) (median 3.5%) (Figure 3A), consistent with XCI-dependent CGI methylation. We then looked at six CGIs identified in *ARHGAP36* and found higher methylation in females than in males, just as in the other X-linked CGIs (Figure 3B). By contrast, the CGIs of known XCI-escaper genes, such as *KDM6A, MED14*, and *DDX3X*,[43] were unmethylated in both sexes (Figure S5C). We then analyzed the allelic methylation status of one of the *ARHGAP36* CGIs where two SNPs were available (A/G and C/A substitutions at positions 109,204,156 and 109,204,409, respectively). The result showed that both alleles are moderately methylated (Figure 3C), consistent with the random XCI in tissues consisting of a heterogeneous cell population, rather than parental-origin-dependent (imprinted) or other types of skewed XCI.[44] Altogether, our results corroborate Lyon's hypothesis that the color patterns of tortoiseshell and calico cats are the results of random XCI of the *O* gene.[8]

Origins of the genetic variations responsible for the coat colors

As described above, all 24 cats with orange coat color that we analyzed had the 5.1-kb deletion (Tables 1 and S1). They were either owned or feral cats, which were mostly from the Fukuoka City area of Japan. Also, 61 of the 258 cats contributed by the 99 Lives Cat Genome Sequencing Initiative[14] (Table S4), which had exactly the same deletion, included those from the United States, Europe, and the Middle East.[45] Thus, in contrast to the

multiple origin hypothesis previously postulated,[11] it is likely that the 5.1-kb deletion is widely distributed in domestic cats worldwide, suggesting a single origin of the orange phenotype.

Calico cats have white coat regions in addition to orange and black-brownish patches. A feline endogenous retrovirus insertion within the *KIT* gene on chromosome B1 has been identified as the causative genetic variation for white spotting (w^s).[42] By PCR genotyping, we found that all of our cats with white coat regions (n = 25), including all 14 calico cats, carried at least one w^s allele (Table S1), consistent with the previous report.[46] In contrast, cats without white coat regions (n = 33), including all six tortoiseshell cats, did not carry this allele (Table S1).

Lastly, the golden hamster (*Mesocricetus auratus*) exhibits orange coloration due to the activity of an X-linked gene designated *Sex-linked yellow* (*Sly*).[47] Using a high-quality chromosome-scale sequence assembly of the golden hamster genome,[48] we examined whether the genomic position of *Arhgap36* corresponds to the genetic location of *Sly*. This analysis showed that the two loci are located in different regions of the X chromosome (Figure S6), supporting the previous conclusion reached by a genetic study that *Sly* and *O* are distinct.[47] Together with the knowledge obtained so far in humans and mice, this result suggests that the genetic contribution of *ARHGAP36* and the UCE-like sequence to orange coloration is unique to certain mammalian species, such as domestic cats.

DISCUSSION

More than 60 years ago, Lyon suggested that the alternative black-brownish and orange patches of tortoiseshell cats are consistent with the random inactivation of the heretofore unidentified X-linked *O* gene in heterozygous females.[8] Our systematic screening now identifies a 5.1-kb deletion within an intron of *ARHGAP36*, which is among the previously listed candidate genes in the *O* haplotype region,[12] as the genetic variation responsible for the orange coloration. Findings similar to ours were recently reported by Kaelin et al.,[49] which, together with ours, support the single origin of the orange phenotype. Although no non-invasive method is available at present for direct demonstration of the causal relationship in this companion animal species, a perfect association between the existence of the genetic variation deleting a putative regulatory element and the orange coloration strongly supports our conclusion. While *ARHGAP36* and its adjacent gene, *IGSF1*, appear to share some regulatory mechanisms, the observed higher expression of the former in the skin, its known roles in signaling pathways related to hair follicle development and melanogenesis (the HH and PKA pathways), and its implications in human skin diseases involving hair follicles and naevi[30] all point to it as an excellent candidate for the long-sought *O* gene. Furthermore, we provide evidence that *ARHGAP36* is subject to XCI in female human and mouse cells. Our results on the allelic DNA methylation status of the *ARHGAP36* CGIs are also consistent with the random inactivation of this gene in female cats.

ARHGAP36 encodes a member of the Rho GTPase-activating protein family and is implicated in neuronal development, bone formation, hair follicle development, and cancer development or progression through positive and negative regulation of the HH and PKA signaling pathways, respectively,[25–30] but no role has been reported in melanogenesis. In fact, no locus affecting hair or coat color has been mapped at the orthologous location in humans or mice. Additionally, our study provides another layer of support for the previous finding that the X-linked *Sly*, which is responsible for the orange coat coloration of the golden hamster, is distinct from the *O* locus.[47] Thus, ARHGAP36 protein is a novel factor regulating the melanogenesis pathway, and this role may be specific to the domestic cat or the feline family members. Consistent with this, our attempts to generate mouse models by introducing the genetic variation have not been successful: neither a deletion corresponding to the one found in domestic cats nor a more targeted deletion restricted to the UCE-like sequence caused any discernible coat color change in several engineered mouse lines.

How does *ARHGAP36* regulate melanogenesis? An immunostaining study previously reported the expression of human *ARHGAP36* in a small number of hair follicle cells in the outer root sheath of healthy skin.[30] On the other hand, according to the public databases, *ARHGAP36* is highly expressed in tissues containing neural crest derivatives, implying that melanocytes, which are also of neural crest origin, could express this gene. In fact, Kaelin et al. recently showed by *in situ* hybridization that *ARHGAP36* is robustly expressed in hair follicle melanocytes from cats carrying the 5.1-kb deletion in a study similar to ours.[49] In any case, our RNA-seq data show that *ARHGAP36* expression in melanocytes, or cells communicating with them, negatively regulates a variety of melanogenesis pathway genes, including those encoding signaling molecules (ligands) and enzymes directly involved in melanin synthesis. It is interesting that the ARHGAP36 protein appears to lack the GTPase-activating activity[24] but has the potential to inhibit PKA signaling directly by blocking the catalytic activity of PKA or by accelerating ubiquitin-mediated degradation of the catalytic subunit of PKA.[26] The second mechanism for PKA inhibition by ARHGAP36 was recently confirmed in a human melanoma model.[49] The PKA signaling elicited by MC1R bound to melanocyte-stimulating hormone is a fundamental pathway regulating melanin synthesis,[50] and, in fact, genetic variations in MC1R are associated with red hair and fair skin in humans (increased pheomelanin and decreased eumelanin).[51] So, if *ARHGAP36* is expressed in melanocytes, it could directly modulate the PKA pathway to alter the balance between eumelanin and pheomelanin.

The genomic region of the 5.1-kb deletion contains a UCE-like sequence containing putative binding sites for transcriptional activators and repressors. Based on the expression patterns of cat *ARHGAP36* in colored coat regions, we speculate that the deletion disrupts its regulated expression and causes inappropriate activation. However, we do not know the precise change caused by the deletion since the follicle melanogenesis is a complex process regulated by a variety of intrinsic and extrinsic factors. For example, it is restricted to the anagen stage of the hair cycle and coupled to the life cycle of melanocytes with changes in their distribution and differentiation.[50] Therefore, we would first need to know the precise regulation of *ARHGAP36* in healthy cat follicles. Since samples required for such a systematic study are not easily accessible in this non-experimental animal species, we are hoping that recently derived feline induced pluripotent stem (iPS) cells[52] and their use in constructing *in vitro* systems, including organoids, would resolve some of the problems. In

CellPress
OPEN ACCESS

particular, the derivation of naive female iPS cells carrying two active X chromosomes and their differentiation into melanocytes and other relevant cells would recapitulate the random XCI and production of different pigment species in different melanocytes. Further investigation warrants a detailed understanding of how the deletion eventually leads to eumelanin to pheomelanin synthesis.

In conclusion, we have identified the X-linked *ARHGAP36* gene as the strong candidate as the long-sought *O* gene of the domestic cat. Although it is not fully understood how the identified deletion switches the pigment species, the variation likely dominates the cat population with orange coat color. We also provide evidence that *ARHGAP36* is most likely subject to random XCI in the domestic cat, as previously suggested by Lyon.[8] How this gene became employed in melanogenesis in certain species and how it exerts pleiotropic biological effects in mammals are interesting future questions.

RESOURCE AVAILABILITY

Lead contact

Further information and requests for resources and reagents should be directed to and will be fulfilled by the lead contact, Hiroyuki Sasaki (hsasaki@bioreg.kyushu-u.ac.jp).

Materials availability

This study did not generate new unique reagents.

Data and code availability

All sequencing data related to this study are publicly available in the DDBJ/ENA/NCBI databases under BioProject no. PRJDB18200. This paper does not report original code. Any additional information required to reanalyze the data reported in this paper is available from the lead contact upon request.

ACKNOWLEDGMENTS

We thank Chaoqing Wen, Junko Oishi, Hiroaki Ohishi, Sangwan Kim, Sayaka Misumi, Masanobu Deshimaru, Yoshihiro Izumi, and Takeshi Bamba for technical assistance; Sei Matsumura and Keiko Akenaga for their help in collecting the cat samples; and Shingo Hatoya, Hiroaki Yamamoto, and Tomohisa Hirobe for valuable discussion. We also thank Naohito Nozaki, Yasuaki Mohri, and Emi Nishimura for their technical advice and the Common Research Facility/Research Promotion Unit of the Medical Institute of Bioregulation, Kyushu University, for technical support. This research project was partly supported by 619 crowdfunding backers on the READYFOR platform (https://readyfor.jp/projects/calico60).

AUTHOR CONTRIBUTIONS

M.U., M.M., and H.S. conceived the study and planned the experiments. M.U., Y. Matsumoto, Y. Matsumura, and M.M. collected the cat samples. W.K.A.Y., M.U., Y. Miki, and M.M. performed the experiments, and H.T., W.K.A.Y., Y.N., and H.S. analyzed the data. Y.B. and T.S. analyzed the data from mouse studies. Y.B., Y.N., M.M., and H.S. supervised the entire project. H.T., W.K.A.Y., M.U., M.M., and H.S. interpreted the results and wrote the paper with input from all authors.

DECLARATION OF INTERESTS

The authors declare no competing interests.

STAR★METHODS

Detailed methods are provided in the online version of this paper and include the following:

- KEY RESOURCES TABLE
- EXPERIMENTAL MODEL AND STUDY PARTICIPANT DETAILS
  - Sampling of domestic cats
- METHOD DETAILS
  - DNA and RNA extraction
  - Genotyping
  - Sanger sequencing
  - WGS, RNA-seq, and WGBS
- QUANTIFICATION AND STATISTICAL ANALYSIS
  - WGS data analysis
  - RNA-seq data analysis
  - WGBS data analysis

SUPPLEMENTAL INFORMATION

Supplemental information can be found online at https://doi.org/10.1016/j.cub.2025.03.075.

Received: December 23, 2024
Revised: March 6, 2025
Accepted: March 28, 2025
Published: May 15, 2025

REFERENCES

1. Driscoll, C.A., Menotti-Raymond, M., Roca, A.L., Hupe, K., Johnson, W.E., Geffen, E., Harley, E.H., Delibes, M., Pontier, D., Kitchener, A.C., et al. (2007). The Near Eastern origin of cat domestication. Science *317*, 519–523. https://doi.org/10.1126/science.1139518.
2. Vigne, J.D., Briois, F., Zazzo, A., Willcox, G., Cucchi, T., Thiébault, S., Carrère, I., Franel, Y., Touquet, R., Martin, C., et al. (2012). First wave of cultivators spread to Cyprus at least 10,600 y ago. Proc. Natl. Acad. Sci. USA *109*, 8445–8449. https://doi.org/10.1073/pnas.1201693109.
3. Ottoni, C., Van Neer, W., De Cupere, B., Daligault, J., Guimaraes, S., Peters, J., Spassov, N., Prendergast, M.E., Boivin, N., Morales-Muñiz, A., et al. (2017). The palaeogenetics of cat dispersal in the ancient world. Nat. Ecol. Evol. *1*, 0139. https://doi.org/10.1038/s41559-017-0139.
4. Doncaster, L. (1904). On the inheritance of tortoiseshell and related colors in cats. Proc. Camb. Philol. Soc. *13*, 35–38.
5. Little, C.C. (1919). Colour inheritance in cats, with special reference to colours, black, yellow and tortoiseshell. J. Genet. *8*, 279–290. https://doi.org/10.1007/BF02983269.
6. Bamber, R.C., and Herdman, E.C. (1927). The inheritance of black, yellow and tortoiseshell coat colour in cats. J. Genet. *18*, 87–97.
7. Vella, C.M., Shelton, L.M., McGonagle, J.J., and Stanglein, T.W. (1999). Robinson's Genetics for Cat Breeders and Veterinarians (Butterworth-Heinemann).
8. Lyon, M.F. (1961). Gene action in the X-chromosome of the mouse (*Mus musculus* L.). Nature *190*, 372–373. https://doi.org/10.1038/190372a0.
9. Moran, C., Gillies, C.B., and Nicholas, F.W. (1984). Fertile male tortoiseshell cats. Mosaicism due to gene instability? J. Hered. *75*, 397–402. https://doi.org/10.1093/oxfordjournals.jhered.a109964.
10. Grahn, R.A., Lemesch, B.M., Millon, L.V., Matise, T., Rogers, Q.R., Morris, J.G., Fretwell, N., Bailey, S.J., Batt, R.M., and Lyons, L.A. (2005). Localizing the X-linked orange colour phenotype using feline resource families. Anim. Genet. *36*, 67–70. https://doi.org/10.1111/j.1365-2052.2005.01239.x.
11. Schmidt-Küntzel, A., Nelson, G., David, V.A., Schäffer, A.A., Eizirik, E., Roelke, M.E., Kehler, J.S., Hannah, S.S., O'Brien, S.J., and Menotti-Raymond, M. (2009). A domestic cat X chromosome linkage map and the sex-linked orange locus: mapping of orange, multiple origins and epistasis over nonagouti. Genetics *181*, 1415–1425. https://doi.org/10.1534/genetics.108.095240.

12. Gandolfi, B., Alhaddad, H., Abdi, M., Bach, L.H., Creighton, E.K., Davis, B.W., Decker, J.E., Dodman, N.H., Ginns, E.I., Grahn, J.C., et al. (2018). Applications and efficiencies of the first cat 63K DNA array. Sci. Rep. *8*, 7024. https://doi.org/10.1038/s41598-018-25438-0.

13. Matsumoto, Y., Yik-Lok Chung, C.Y.L., Isobe, S., Sakamoto, M., Lin, X., Chan, T.F., Hirakawa, H., Ishihara, G., Lam, H.M., Nakayama, S., et al. (2024). Chromosome-scale assembly with improved annotation provides insights into breed-wide genomic structure and diversity in domestic cats. J. Adv. Res. https://doi.org/10.1016/j.jare.2024.10.023.

14. Lyons, L.A., Buckley, R.M., and Harvey, R.J.; 99 Lives Cat Genome Consortium (2021). Mining the 99 Lives Cat Genome Sequencing Consortium database implicates genes and variants for the Ticked locus in domestic cats (*Felis catus*). Anim. Genet. *52*, 321–332. https://doi.org/10.1111/age.13059.

15. Hernandez, I., Hayward, J.J., Brockman, J.A., White, M.E., Moutham, L., Wilcox, E.A., Garrison, S., Castelhano, M.G., Loftus, J.P., Gomes, F.E., et al. (2022). Complex feline disease mapping using a dense genotyping array. Front. Vet. Sci. *9*, 862414. https://doi.org/10.3389/fvets.2022.862414.

16. Bejerano, G., Pheasant, M., Makunin, I., Stephen, S., Kent, W.J., Mattick, J.S., and Haussler, D. (2004). Ultraconserved elements in the human genome. Science *304*, 1321–1325. https://doi.org/10.1126/science.1098119.

17. ENCODE Project Consortium (2012). An integrated encyclopedia of DNA elements in the human genome. Nature *489*, 57–74. https://doi.org/10.1038/nature11247.

18. Tremblay, M., Sanchez-Ferras, O., and Bouchard, M. (2018). GATA transcription factors in development and disease. Development *145*, dev164384. https://doi.org/10.1242/dev.164384.

19. Erichsen, D.A., Armstrong, M.B., and Wechsler, D.S. (2015). Mxi1 and mxi1-0 antagonize N-myc function and independently mediate apoptosis in neuroblastoma. Transl. Oncol. *8*, 65–74. https://doi.org/10.1016/j.tranon.2015.01.002.

20. Rivera, C., Lee, H.G., Lappala, A., Wang, D., Noches, V., Olivares-Costa, M., Sjöberg-Herrera, M., Lee, J.T., and Andrés, M.E. (2022). Unveiling RCOR1 as a rheostat at transcriptionally permissive chromatin. Nat. Commun. *13*, 1550. https://doi.org/10.1038/s41467-022-29261-0.

21. GTEx Consortium. (2013). The Genotype-Tissue Expression (GTEx) project. Nat. Genet. *45*, 580–585. https://doi.org/10.1038/ng.2653.

22. Mort, R.L., Jackson, I.J., and Patton, E.E. (2015). The melanocyte lineage in development and disease. Development *142*, 620–632. https://doi.org/10.1242/dev.106567.

23. Sun, Y., Bak, B., Schoenmakers, N., van Trotsenburg, A.S.P., Oostdijk, W., Voshol, P., Cambridge, E., White, J.K., le Tissier, P., Gharavy, S.N.M., et al. (2012). Loss-of-function mutations in *IGSF1* cause an X-linked syndrome of central hypothyroidism and testicular enlargement. Nat. Genet. *44*, 1375–1381. https://doi.org/10.1038/ng.2453.

24. Müller, P.M., Rademacher, J., Bagshaw, R.D., Wortmann, C., Barth, C., van Unen, J., Alp, K.M., Giudice, G., Eccles, R.L., Heinrich, L.E., et al. (2020). Systems analysis of RhoGEF and RhoGAP regulatory proteins reveals spatially organized RAC1 signalling from integrin adhesions. Nat. Cell Biol. *22*, 498–511. https://doi.org/10.1038/s41556-020-0488-x.

25. Rack, P.G., Ni, J., Payumo, A.Y., Nguyen, V., Crapster, J.A., Hovestadt, V., Kool, M., Jones, D.T.W., Mich, J.K., Firestone, A.J., et al. (2014). Arhgap36-dependent activation of Gli transcription factors. Proc. Natl. Acad. Sci. USA *111*, 11061–11066. https://doi.org/10.1073/pnas.1322362111.

26. Eccles, R.L., Czajkowski, M.T., Barth, C., Müller, P.M., McShane, E., Grunwald, S., Beaudette, P., Mecklenburg, N., Volkmer, R., Zühlke, K., et al. (2016). Bimodal antagonism of PKA signalling by ARHGAP36. Nat. Commun. *7*, 12963. https://doi.org/10.1038/ncomms12963.

27. Nam, H., Jeon, S., An, H., Yoo, J., Lee, H.J., Lee, S.K., and Lee, S. (2019). Critical roles of ARHGAP36 as a signal transduction mediator of Shh pathway in lateral motor columnar specification. Elife *8*, e46683. https://doi.org/10.7554/eLife.46683.

28. Zhang, B., Zhuang, T., Lin, Q., Yang, B., Xu, X., Xin, G., Zhu, S., Wang, G., Yu, B., Zhang, T., et al. (2019). Patched1-ArhGAP36-PKA-Inversin axis determines the ciliary translocation of Smoothened for Sonic Hedgehog pathway activation. Proc. Natl. Acad. Sci. USA *116*, 874–879. https://doi.org/10.1073/pnas.1804042116.

29. Melo, U.S., Jatzlau, J., Prada-Medina, C.A., Flex, E., Hartmann, S., Ali, S., Schöpflin, R., Bernardini, L., Ciolfi, A., Moeinzadeh, M.H., et al. (2023). Enhancer hijacking at the *ARHGAP36* locus is associated with connective tissue to bone transformation. Nat. Commun. *14*, 2034. https://doi.org/10.1038/s41467-023-37585-8.

30. Liu, Y., Banka, S., Huang, Y., Hardman-Smart, J., Pye, D., Torrelo, A., Beaman, G.M., Kazanietz, M.G., Baker, M.J., Ferrazzano, C., et al. (2022). Germline intergenic duplications at Xq26.1 underlie Bazex-Dupré-Christol basal cell carcinoma susceptibility syndrome. Br. J. Dermatol. *187*, 948–961. https://doi.org/10.1111/bjd.21842.

31. Kanehisa, M., and Goto, S. (2000). KEGG: kyoto encyclopedia of genes and genomes. Nucleic Acids Res. *28*, 27–30. https://doi.org/10.1093/nar/28.1.27.

32. Huang, D.W., Sherman, B.T., and Lempicki, R.A. (2009). Systematic and integrative analysis of large gene lists using DAVID bioinformatics resources. Nat. Protoc. *4*, 44–57. https://doi.org/10.1038/nprot.2008.211.

33. Snyman, M., Walsdorf, R.E., Wix, S.N., and Gill, J.G. (2024). The metabolism of melanin synthesis—From melanocytes to melanoma. Pigment Cell Melanoma Res. *37*, 438–452. https://doi.org/10.1111/pcmr.13165.

34. Carrel, L., and Willard, H.F. (2005). X-inactivation profile reveals extensive variability in X-linked gene expression in females. Nature *434*, 400–404. https://doi.org/10.1038/nature03479.

35. Sakakibara, Y., Nagao, K., Blewitt, M., Sasaki, H., Obuse, C., and Sado, T. (2018). Role of SmcHD1 in establishment of epigenetic states required for the maintenance of the X-inactivated state in mice. Development *145*, dev166462. https://doi.org/10.1242/dev.166462.

36. Ichihara, S., Nagao, K., Sakaguchi, T., Obuse, C., and Sado, T. (2022). SmcHD1 underlies the formation of H3K9me3 blocks on the inactive X chromosome in mice. Development *149*, dev200864. https://doi.org/10.1242/dev.200864.

37. Gdula, M.R., Nesterova, T.B., Pintacuda, G., Godwin, J., Zhan, Y., Ozadam, H., McClellan, M., Moralli, D., Krueger, F., Green, C.M., et al. (2019). The non-canonical SMC protein SmcHD1 antagonises TAD formation and compartmentalisation on the inactive X chromosome. Nat. Commun. *10*, 30. https://doi.org/10.1038/s41467-018-07907-2.

38. Cotton, A.M., Ge, B., Light, N., Adoue, V., Pastinen, T., and Brown, C.J. (2013). Analysis of expressed SNPs identifies variable extents of expression from the human inactive X chromosome. Genome Biol. *14*, R122. https://doi.org/10.1186/gb-2013-14-11-r122.

39. Cotton, A.M., Price, E.M., Jones, M.J., Balaton, B.P., Kobor, M.S., and Brown, C.J. (2015). Landscape of DNA methylation on the X chromosome reflects CpG density, functional chromatin state and X-chromosome inactivation. Hum. Mol. Genet. *24*, 1528–1539. https://doi.org/10.1093/hmg/ddu564.

40. Duncan, C.G., Grimm, S.A., Morgan, D.L., Bushel, P.R., Bennett, B.D., NISC Comparative Sequencing Program, Roberts, J.D., Tyson, F.L., Merrick, B.A., and Wade, P.A. (2018). Dosage compensation and DNA methylation landscape of the X chromosome in mouse liver. Sci. Rep. *8*, 10138. https://doi.org/10.1038/s41598-018-28356-3.

41. Toh, H., Okae, H., Shirane, K., Sato, T., Hamada, H., Kikutake, C., Saito, D., Arima, T., Sasaki, H., and Suyama, M. (2024). Epigenetic dynamics of partially methylated domains in human placenta and trophoblast stem cells. BMC Genomics *25*, 1050. https://doi.org/10.1186/s12864-024-10986-9.

42. Tamazian, G., Simonov, S., Dobrynin, P., Makunin, A., Logachev, A., Komissarov, A., Shevchenko, A., Brukhin, V., Cherkasov, N., Svitin, A., et al. (2014). Annotated features of domestic cat - *Felis catus* genome. Gigascience *3*, 13. https://doi.org/10.1186/2047-217X-3-13.

43. Balaton, B.P., Fornes, O., Wasserman, W.W., and Brown, C.J. (2021). Cross-species examination of X-chromosome inactivation highlights

domains of escape from silencing. Epigenetics Chromatin *14*, 12. https://doi.org/10.1186/s13072-021-00386-8.

44. Furlan, G., and Galupa, R. (2022). Mechanisms of choice in X-chromosome inactivation. Cells *11*, 535. https://doi.org/10.3390/cells11030535.
45. Buckley, R.M., Davis, B.W., Brashear, W.A., Farias, F.H.G., Kuroki, K., Graves, T., Hillier, L.W., Kremitzki, M., Li, G., Middleton, R.P., et al. (2020). A new domestic cat genome assembly based on long sequence reads empowers feline genomic medicine and identifies a novel gene for dwarfism. PLoS Genet. *16*, e1008926. https://doi.org/10.1371/journal.pgen.1008926.
46. David, V.A., Menotti-Raymond, M., Wallace, A.C., Roelke, M., Kehler, J., Leighty, R., Eizirik, E., Hannah, S.S., Nelson, G., Schäffer, A.A., et al. (2014). Endogenous retrovirus insertion in the *KIT* oncogene determines *white* and *white spotting* in domestic cats. G3 (Bethesda) *4*, 1881–1891. https://doi.org/10.1534/g3.114.013425.
47. Alizadeh, A., Hong, L.Z., Kaelin, C.B., Raudsepp, T., Manuel, H., and Barsh, G.S. (2009). Genetics of *Sex-linked yellow* in the Syrian hamster. Genetics *181*, 1427–1436. https://doi.org/10.1534/genetics.108.095018.
48. Ishino, K., Hasuwa, H., Yoshimura, J., Iwasaki, Y.W., Nishihara, H., Seki, N.M., Hirano, T., Tsuchiya, M., Ishizaki, H., Masuda, H., et al. (2021). Hamster PIWI proteins bind to piRNAs with stage-specific size variations during oocyte maturation. Nucleic Acids Res. *49*, 2700–2720. https://doi.org/10.1093/nar/gkab059.
49. Kaelin, C.B., McGowan, K.A., Trotman, J.C., Koroma, D.C., David, V.A., Menotti-Raymond, M., Graff, E.C., Schmidt-Küntzel, A., Oancea, E., and Barsh, G.S. (2024). Molecular and genetic characterization of sex-linked orange coat color in the domestic cat. Preprint at bioRxiv, 2024.11.21.624608 . https://doi.org/10.1101/2024.11.21.624608.
50. Slominski, A., Wortsman, J., Plonka, P.M., Schallreuter, K.U., Paus, R., and Tobin, D.J. (2005). Hair follicle pigmentation. J. Invest. Dermatol. *124*, 13–21. https://doi.org/10.1111/j.0022-202X.2004.23528.x.
51. Valverde, P., Healy, E., Jackson, I., Rees, J.L., and Thody, A.J. (1995). Variants of the melanocyte-stimulating hormone receptor gene are associated with red hair and fair skin in humans. Nat. Genet. *11*, 328–330. https://doi.org/10.1038/ng1195-328.
52. Kimura, K., Tsukamoto, M., Sugisaki, H., Tanaka, M., Kuwamura, M., Matsumoto, Y., Ishihara, G., Watanabe, K., Okada, M., Nakanishi, M., et al. (2024). Generation of footprint-free, high-quality feline induced pluripotent stem cells using Sendai virus vector. Regen. Ther. *26*, 708–716. https://doi.org/10.1016/j.reth.2024.08.012.
53. Li, H., and Durbin, R. (2009). Fast and accurate short read alignment with Burrows-Wheeler transform. Bioinformatics *25*, 1754–1760. https://doi.org/10.1093/bioinformatics/btp324.
54. Van der Auwera, G.A., Carneiro, M.O., Hartl, C., Poplin, R., Del Angel, G., Levy-Moonshine, A., Jordan, T., Shakir, K., Roazen, D., Thibault, J., et al. (2013). From FastQ data to high confidence variant calls: the genome analysis toolkit best practices pipeline. Curr. Protoc. Bioinformatics *43*, 11.10.1–11.10.33. https://doi.org/10.1002/0471250953.bi1110s43.
55. Cingolani, P., Platts, A., Wang, L.L., Coon, M., Nguyen, T., Wang, L., Land, S.J., Lu, X., and Ruden, D.M. (2012). A program for annotating and predicting the effects of single nucleotide polymorphisms, SnpEff: SNPs in the genome of *Drosophila melanogaster* strain w1118; iso-2; iso-3. Fly *6*, 80–92. https://doi.org/10.4161/fly.19695.
56. Kim, D., Langmead, B., and Salzberg, S.L. (2015). HISAT: a fast spliced aligner with low memory requirements. Nat. Methods *12*, 357–360. https://doi.org/10.1038/nmeth.3317.
57. Pertea, M., Pertea, G.M., Antonescu, C.M., Chang, T.C., Mendell, J.T., and Salzberg, S.L. (2015). StringTie enables improved reconstruction of a transcriptome from RNA-seq reads. Nat. Biotechnol. *33*, 290–295. https://doi.org/10.1038/nbt.3122.
58. Krueger, F., and Andrews, S.R. (2011). Bismark: a flexible aligner and methylation caller for Bisulfite-Seq applications. Bioinformatics *27*, 1571–1572. https://doi.org/10.1093/bioinformatics/btr167.
59. Krueger, F., and Andrews, S.R. (2016). SNPsplit: Allele-specific splitting of alignments between genomes with known SNP genotypes. F1000Res *5*, 1479. https://doi.org/10.12688/f1000research.9037.2.
60. Miura, F., Enomoto, Y., Dairiki, R., and Ito, T. (2012). Amplification-free whole-genome bisulfite sequencing by post-bisulfite adaptor tagging. Nucleic Acids Res. *40*, e136. https://doi.org/10.1093/nar/gks454.
61. Frazer, K.A., Pachter, L., Poliakov, A., Rubin, E.M., and Dubchak, I. (2004). VISTA: computational tools for comparative genomics. Nucleic Acids Res. *32*, W273–W279. https://doi.org/10.1093/nar/gkh458.
62. Larkin, M.A., Blackshields, G., Brown, N.P., Chenna, R., McGettigan, P.A., McWilliam, H., Valentin, F., Wallace, I.M., Wilm, A., Lopez, R., et al. (2007). Clustal W and Clustal X version 2.0. Bioinformatics *23*, 2947–2948. https://doi.org/10.1093/bioinformatics/btm404.
63. Gardiner-Garden, M., and Frommer, M. (1987). CpG islands in vertebrate genomes. J. Mol. Biol. *196*, 261–282. https://doi.org/10.1016/0022-2836(87)90689-9.

STAR★METHODS

KEY RESOURCES TABLE

REAGENT or RESOURCE	SOURCE	IDENTIFIER
Biological samples		
Domestic cat blood	Inakazu Dog & Cat Kashii Hospital	https://www.inakazu-vet.com/
Domestic cat ovary	Cat clinics in Japan	N/A
Domestic cat auricular	Cat clinics in Japan	N/A
Critical commercial assays		
EZ DNA Methylation-Gold	Zymo Research	D5005
NEBNext rRNA Depletion Kit (Human/Mouse/Rat)	NEB	E6310L
NEBNext Ultra II Directional RNA Library Prep Kit for Illumina	NEB	E7760S
NucleoSpin Blood kit	Macherey-Nagel	740951.10
TruSeq DNA PCR-Free LT Library Prep Kit	Illumina	FC-121-3001
Deposited data		
Fastq files from WGS, RNA-seq, and WGBS	This paper	BioProject: PRJDB18200
Domestic cat reference genome AnAms1.0	Matsumoto et al.[13]	https://cat.annotation.jp/
WGS data from domestic cats	99 Lives Cat Genome Sequencing Initiative	Shown in Table S4 of this paper
Gene expression microarray (BeadChip) data from human lymphoblastoid cell lines	Cotton et al.[38]	GEO: GSE26286
RNA-seq data from mouse embryonic fibroblasts	Sakakibara et al.[35]	GEO: GSE112097
RNA-seq data from mouse embryonic fibroblasts	Gdula et al.[37]	GEO: GSE121184
RNA-seq data from domestic cats	99 Lives Cat Genome Sequencing Initiative	BioProject: PRJNA312519
WGBS data from a male cat Boris	Tamazian et al.[42]	SRA: SRX548709
WGBS data from human cytotrophoblasts	Toh et al.[41]	NBDC: hum0086
WGBS data from mouse liver	Duncan et al.[40]	GEO: GSE106379
WGBS data from mouse embryonic fibroblasts	Gdula et al.[37]	GEO: GSE122094
Golden hamster genome sequence	Ishino et al.[48]	SRA: DRA010879
Oligonucleotides		
Primer: *ARHGAP36* F1 GAAATACCTATGCTAGCCGTC	This paper	N/A
Primer: *ARHGAP36* R1 TGTGTGGTACACATGATTTCAG	This paper	N/A
Primer: *ARHGAP36* F2 TGGTGTCTGCTTCTGCACCT	This paper	N/A
Primer: *ARHGAP36* R2 AAACAGGAAATGGTCCATATGC	This paper	N/A
Primer: *SRY* F1 AAGATGATAAGTTGGTGGCTC	This paper	N/A
Primer: *SRY* R1 GGCCACTCTTTGCGACAAC	This paper	N/A
Primer: *KIT* F1 TCAGGAGCCTGCAAATCCTC	This paper	N/A

(*Continued on next page*)

CellPress
OPEN ACCESS

Continued

REAGENT or RESOURCE	SOURCE	IDENTIFIER
Primer: *KIT* R1 CGCTGGAACGCTCAGGTCTTC	This paper	N/A
Primer: *KIT* F2 TGGTATCTCACCGCTGCGTC	This paper	N/A
Software and algorithms		
BWA v0.7.17	Li et al.[53]	https://bio-bwa.sourceforge.net/
GATK v4.1.3	Van der Auwera et al.[54]	https://gatk.broadinstitute.org/
SnpEff v4.3	Cingolani et al.[55]	https://pcingola.github.io/SnpEff/
HISAT2 v2.0.5	Kim et al.[56]	https://daehwankimlab.github.io/hisat2/
StringTie v2.1.4	Pertea et al.[57]	https://www.ccb.jhu.edu/software/stringtie/
DAVID	Huang et al.[32]	https://davidbioinformatics.nih.gov/
Bismark v0.10.0	Krueger et al.[58]	https://www.bioinformatics.babraham.ac.uk/projects/bismark/
SNPsplit v0.3.2	Krueger et al.[59]	https://www.bioinformatics.babraham.ac.uk/projects/SNPsplit/
Other		
TRIzol Reagent	Thermo Fisher Scientific	15596026
KOD One PCR Master Mix	TOYOBO	18538-01
BigDye Terminator v3.1	Thermo Fisher Scientific	4337455
Klenow Fragment (3′ →5′ exo-)	NEB	M0212M
Bst DNA Polymerase Large Fragment	NEB	M0275S
Phusion Hot Start II DNA Polymerase	Thermo Fisher Scientific	F549L

EXPERIMENTAL MODEL AND STUDY PARTICIPANT DETAILS

Sampling of domestic cats

Sampling of domestic cats was carried out in accordance with the ethical guidelines of Kyushu University using the protocols approved by the Animal Experiment Committee (#A21-433-1). Blood samples and small tissue pieces were acquired by veterinarians during routine veterinary practice or spaying/neutering surgery. Skin tissues from an animal that died of unknown causes were voluntarily donated by a breeder. Samples were collected from two different skin regions of each coat color in cat #01 (see Figure S1C). Skin fragments of 2 mm square including dermis and epidermis but excluding subcutaneous tissues were collected from each coat color region, carefully avoiding areas with different fur colors.

METHOD DETAILS

DNA and RNA extraction

Genomic DNA was extracted from whole blood cells using the NucleoSpin Blood kit (Macherey-Nagel) or from tissue samples by a standard method involving proteinase K digestion and isopropanol precipitation. Total RNA was extracted from tissue samples using TRIzol Reagent (Thermo Fisher Scientific).

Genotyping

The cats were genotyped for alleles of *ARHGAP36* (Δ/+) and *KIT* (w^+/w^s) by PCR using KOD One PCR Master Mix (TOYOBO) with primers listed in key resources table. Some animals were also examined for the presence of *SRY* on the Y chromosome.

Sanger sequencing

Sanger sequencing of PCR products was performed to determine the exact position and size of the deletion using BigDye Terminator v3.1 (Thermo Fisher Scientific) and primers listed in key resources table.

WGS, RNA-seq, and WGBS

WGS libraries were prepared from genomic DNA using the TruSeq DNA PCR-Free LT Library Prep Kit (Illumina) and sequenced to generate 53-nt paired-end reads on an Illumina NovaSeq 6000 equipped with NVCS v1.6.0 and RTA v3.4.4. RNA-seq libraries were prepared from total RNA using NEBNext rRNA Depletion Kit, NEBNext Ultra II Directional RNA Library Prep Kit for Illumina, and NEBNext Multiplex Oligos for Illumina (96 Unique Dual Index Primer Pairs) (NEB). Sequencing was performed using a SP Reagent

Kit (Illumina) on an Illumina NovaSeq 6000 equipped with NVCS v1.6.0 and RTA v3.4.4 to generate 53-nt paired-end reads. WGBS libraries were prepared using the post-bisulfite adapter tagging method.[60] Two hundred ng of genomic DNA spiked with 2 ng lambda phage DNA (Promega) was subjected to bisulfite conversion using EZ Methylation-Gold Kit (Zymo Research). The bisulfite converted DNA was then subjected to two rounds of random priming with N4 primers followed by sequential enzymatic reactions with Klenow Fragment (3'->5' exo-, NEB), Bst DNA Polymerase Large Fragment (NEB), and Phusion Hot Start II DNA Polymerase (Thermo Fisher Scientific). Sequencing was performed using a S1 Reagent Kit (Illumina) on an Illumina NovaSeq 6000 equipped with NVCS v1.6.0 and RTA v3.4.4 to generate 108-nt single-end reads. All read sequences obtained by WGS, RNA-seq, and WGBS were mapped to the domestic cat reference genome (AnAms1.0) obtained from the Cats-I database.[13]

QUANTIFICATION AND STATISTICAL ANALYSIS

WGS data analysis

All paired-end reads were aligned to the AnAms1.0 genome using the Burrows-Wheeler Aligner (BWA v0.7.17)[53] with the BWA-MEM algorithm. Reads mapped to the X chromosome were extracted for further analysis. Duplicate reads were removed using Picard and only uniquely mapped reads were retained. Variant calling was performed using the HaplotypeCaller module of the Genome Analysis Toolkit (GATK v4.1.3)[54] for single nucleotide variants and small insertions and deletions. Variants within the 1.5-Mb haplotype region with a sequencing depth of at least three were extracted from the generated VCF files. To evaluate their potential functional impact, SnpEff v4.3[55] was used, and filtered variants were classified as HIGH or MODERATE impact. Variant profiles were then compared between sample groups with and without the orange coat color to identify orange-specific variants. For genomes lacking the 5.1-kb region, paired-end reads were mapped at intervals of approximately 5,000 bases, compared to the typical mapping distance of 400 bases. This extended read span was used as an indicator of deletion. Raw fastq files from published WGS datasets of 258 cats, including nine with clear color images, contributed primarily by the 99 Lives Cat Genome Sequencing Initiative,[14,45] were obtained from the Sequence Read Archive. The datasets were analyzed using our pipeline described above. Human (hg38 and hg19) and mouse (mm10) X chromosome sequences and ENCODE data were downloaded from the UCSC Genome Browser. Sequence alignment between multiple mammalian species was performed using mVISTA[61] and ClustalW v2.1.[62] The golden hamster genome sequence was obtained from the Sequence Read Archive (DRA010879).[48]

RNA-seq data analysis

Adapter sequences and low-quality bases (Q-score < 30) were removed from the 5′ and 3′ ends using Trim Galore v0.6.0. Paired-end reads longer than 35 bases were retained for analysis. The filtered reads were then aligned to the AnAms1.0 genome by HISAT2 v2.0.5.[56] Transcripts were assembled using StringTie v2.1.4.[57] To characterize the gene regulatory network involving *ARHGAP36*, we identified genes that showed positive and negative correlation with *ARHGAP36* expression in skin samples from a calico cat (#01). Only the orange and black-brownish regions (n = 2 each) were used for the analysis because we did not expect melanogenesis in the white regions. (Indeed, we observed no *ARHGAP36* expression in the white region.) We then grouped the four datasets into two, *ARHGAP36* positive (two orange and one black-brownish samples) and *ARHGAP36* negative (one black-brownish sample). Then, a gene was considered to be positively correlated if its FPKM value was greater than 1 and at least five times higher in all three *ARHGAP36*-positive samples compared with the *ARHGAP36*-negative sample. Conversely, a gene was considered to be negatively correlated if its FPKM was greater than 1 and at least five times higher in the *ARHGAP36*-negtive sample compared to the *ARHGAP36*-positive samples. Then, genes positively and negatively correlated with *ARHGAP36* were subjected to the KEGG pathway analysis using DAVID.[31,32] RNA-seq data from mouse embryonic fibroblasts (GSE112097 and GSE121184)[35,37] were reprocessed as described in the original manuscript for SNP-based allelic expression analysis of mouse *Arhgap36*. RNA-seq data from various cat organs and tissues were acquired from the publicly available dataset (PRJNA312519) and processed using the aforementioned pipeline.

WGBS data analysis

Four bases were removed from the 5′ end of each read, and low-quality bases (Q-score < 30) from the 3′ end. Reads longer than 50 bases were retained for analysis. The filtered reads were then aligned to the AnAms1.0 genome using Bismark v0.10.0[58] with a seed length of 28, allowing a maximum of one mismatch in the seed and enabling the "–pbat" option. Only uniquely aligned reads were used in the subsequent analysis. Data from both DNA strands were combined. Bisulfite conversion rate was estimated using reads uniquely aligned to the lambda phage genome. For allele-specific analysis, reads were separated and grouped based on SNPs present in a *ARHGAP36* CGI using SNPsplit v0.3.2.[59] Then methylated and unmethylated CpGs were individually counted in reads representing each allele and the methylation level was calculated based on the counts. Publicly available WGBS datasets were obtained from the Sequence Read Archive for a male cat named Boris (SRX548709),[42] human cytotrophoblasts (NBDC No. hum0086),[41] and mouse liver (GSE106379).[40] These data were processed using the same pipeline as the cat data analysis. In addition, pre-calculated bedGraph files on DNA methylation of mouse embryonic fibroblasts were obtained from the NCBI Gene Expression Omnibus (GSE122094).[37] CGIs were predicted in the AnAms1.0 genome sequence using the method described by Gardiner-Garden and Frommer.[63] The criteria for CGI identification included a minimum length of 200 bases, a GC content of at least 50%, and an observed to expected CpG ratio (Obs/Exp) of at least 0.6.